Calculation of relaxation rates from microscopic equations of motion

Roger Haydock
Department of Physics and Materials Science Institute, University of Oregon, Eugene, Oregon 97403-1274

C. M. M. Nex and B. D. Simons
Cavendish Laboratory, Madingley Road, Cambridge CB3 0HE, United Kingdom

(Received 9 June 1998)

For classical systems with anharmonic forces, Newton's equations for particle trajectories are nonlinear, while Liouville's equation for the evolution of functions of position and momentum is linear and is solved by constructing a basis of functions in which the Liouvillian is a tridiagonal matrix, which is then diagonalized. For systems that are chaotic in the sense that neighboring trajectories diverge exponentially, the initial conditions determine the solution to Liouville's equation for short times; but for long times, the solutions decay exponentially at rates independent of the initial conditions. These are the relaxation rates of irreversible processes, and they arise in these calculations as the imaginary parts of the frequencies where there are singularities in the analytic continuations of solutions to Liouville's equation. These rates are calculated for two examples: the inverted oscillator, which can be solved both analytically and numerically, and a charged particle in a periodic magnetic field, which can only be solved numerically. In these systems, dissipation arises from traveling-wave solutions to Liouville's equation that couple low and high wave-number modes allowing energy to flow from disturbances that are coherent over large scales to disturbances on ever smaller scales finally becoming incoherent over microscopic scales. These results suggest that dissipation in large scale motion of the system is a consequence of chaos in the small scale motion. [S1063-651X(99)07405-X]

PACS number(s): 05.45.−a, 82.20.Mj, 02.70.−c

I. FROM MICROSCOPIC TO MACROSCOPIC

Although the classical equations of motion for microscopic particles such as atoms and molecules conserve energy exactly, the macroscopic motion of systems of these particles does not. Macroscopic disturbances evolve into smaller and smaller disturbances until the energy of these disturbances is dissipated into incoherent microscopic motion, and the system is in equilibrium. This difference between macroscopic and the microscopic mechanics illustrates one of the difficulties in extracting macroscopic quantities from microscopic equations of motion, namely, that the dissipation, which is central to macroscopic mechanics, arises from disorganized motion on a microscopic scale. Other difficulties include the large number of interacting microscopic degrees of freedom compared to the relatively few macroscopic degrees of freedom, which describe the system.

The purpose of this paper is to show how macroscopic quantities, including those that involve dissipation, can be calculated in a practical way from microscopic equations of motion. The basic idea of our approach is to describe the microscopic mechanics by a linear equation, Liouville's equation [1] in the case of classical mechanics that is the focus of this paper and Schrödinger's equation in the case of quantum mechanics, see further in [2]. Starting with a function describing some initial state of the system, additional functions are constructed to form the basis for a tridiagonal matrix representation of the equation of motion. Diagonalization of the tridiagonal matrix yields the frequencies that dominate at long times and, if these are complex, then their imaginary part is the rate of relaxation to equilibrium.

As examples, we study two systems, the inverted oscillator, chosen because it is analytically tractable, and a charged particle moving in a plane through a perpendicular, periodic magnetic field, chosen because it is numerically tractable. Each system is uniformly hyperbolic in the sense that small changes in the initial positions and momenta of particles lead to exponentially increasing differences in position and momentum. Instead of calculating the trajectories of the particles, we calculate the evolution of functions of position and momentum, and, in particular, it is the overlap of the initial function and the evolved function, the autocorrelation, which describes how quickly the initial state of the system decays.

We find two regimes in the time dependence of the autocorrelation: the first is for short or microscopic times, multiples of some time scale such as a collision time, where the autocorrelation depends sensitively on the initial distribution, and the second is in the limit of infinite time, macroscopic times, where the autocorrelation is independent of the details of the initial distribution. The technical challenge in these calculations is to extract the macroscopic relaxation rates from the complexity and instability of the microscopic motion. Although both examples are of microscopic systems, we find that energy flows from long length scales to short length scales, consistent with dissipation in macroscopic systems.

The flow of energy from long to short length scales, which produces the relaxation at macroscopic times, arises in our calculations from traveling-wave solutions to Liouville's equation which link low-wave-number and high-wave-number functions of position and momentum. The existence of traveling waves depends first on there being an infinite number of nearly degenerate degrees of freedom. Although these systems are spatially finite, there are still an infinite number of independent functions of position and momentum, which have the same time dependence. The different func-

tions simply pack more and more zeros into the same ranges of position and momentum, or in other words, they have larger and larger wave numbers in position and momentum. The second requirement for traveling-wave solutions is that the frequency spectrum of autocorrelation be smooth rather than concentrated at a few frequencies. This latter requirement is met by uniformly hyperbolic systems where particles never repeat, even approximately, their previous trajectories; and so there are no real, singular frequencies in their motion.

After discussing the general solution of Liouville's equation by tridiagonalization in Sec. II, we argue in Sec. III that after macroscopic times, the evolution of the system is governed by the analytic continuation of the microscopic solutions from real to complex frequencies. The development of a practical method for carrying out this analytic continuation is our main result. In Secs. IV and V we illustrate the method, particularly the analytic continuation, for the inverted oscillator and the charge in a periodic magnet, and in Sec. VI we describe how similar calculations could be carried out for larger systems and draw a conclusion about the relation between chaos and dissipation.

II. RECURSIVE SOLUTION OF THE MICROSCOPIC EQUATIONS OF MOTION

The recursive solution of Liouville's equation is described in a previous publication [3], so here we just establish the main results. Instead of attempting to solve the generally nonlinear equations for the trajectories of atoms and molecules, we consider the time evolution of functions on phase space, the space whose coordinates are the positions and momenta of each of the particles. Functions on phase space satisfy a linear equation of motion, Liouville's equation, which relates each function to its time derivative by an operator we call the Liouvillian. Starting with an initial function, we construct a sequence of functions in terms of which the Liouvillian is a tridiagonal matrix. Taking advantage of the tridiagonal form of the Liouvillian, we expand the solution to Liouville's equation in the orthogonal polynomials and the continued fraction associated with the tridiagonal matrix.

For a system of N particles, let Q be a vector whose $3N$ components are the position coordinates of all the particles, and let P be a vector whose $3N$ components are the momenta of all the particles. Newton's law of motion states that the time derivative of each particle's momentum is the force on that particle,

$$dP/dt = F(Q,P), \tag{1}$$

which can depend on the momenta as well as the positions. The rate of change of Q is just the velocity,

$$dQ/dt = V(Q,P), \tag{2}$$

which can in general depend on the positions as well as the momenta. With few exceptions these equations are nonlinear and, therefore, difficult to solve.

We can transform the nonlinear problem of calculating the evolution of Q and P, into the linear problem of calculating the evolution of a function $u(Q,P;t)$ by using the chain rule for differentiation with respect to time, and the constraint that the particles carry the function with them. This leads to Liouville's equation,

$$i\partial u(Q,P;t)/\partial t = -i[V(Q,P)\cdot\nabla_Q u(Q,P;t) + F(Q,P)\cdot\nabla_P u(Q,P;t)], \tag{3}$$

where the total time derivative of $u(Q,P;t)$ is zero and the chain rule generates the scalar products of the time derivative of Q, the velocity, with the Q gradient of $u(Q,P;t)$, and of the time derivative of P, the force, with the P gradient of $u(Q,P;t)$. The factor of i on each side of the equation makes the Liouvillian operator,

$$L = -i[V(Q,P)\cdot\nabla_Q + F(Q,P)\cdot\nabla_P], \tag{4}$$

Hermitian with respect to the inner product between functions $f(Q,P)$ and $g(Q,P)$, defined as

$$\langle f,g\rangle = \int dQ \int dP f(Q,P)^* g(Q,P). \tag{5}$$

When there is a Hamiltonian function, the Liouvillian operator is $-i$ times the Poisson bracket of the Hamiltonian.

Formally, the exponential of the Liouvillian applied to the function at $t=0$, $u(Q,P;0)$, solves Eq. (3) to give

$$u(Q,P;t) = \exp\{-iLt\}u(Q,P;0). \tag{6}$$

It is computationally convenient to express this in terms of the resolvent operator, $(\omega - L)^{-1}$, using the residue theorem,

$$u(Q,P;t) = (1/2\pi i)\int d\omega \exp\{-i\omega t\}(\omega - L)^{-1}u(Q,P;0), \tag{7}$$

where the integral encloses the real ω axis to include the real spectrum of the Liouvillian. Because L is Hermitian with respect to the inner product defined in Eq. (5), $u(Q,P;0)$ can be decomposed into a sum of orthogonal solutions to the time-independent Liouville equation,

$$L\psi_\omega(Q,P) = \omega\psi_\omega(Q,P), \tag{8}$$

of which, at most, one function $\psi_\omega(Q,P)$ is needed for each value of ω. The expression becomes even simpler if the solutions to Eq. (8) are normalized so that

$$\langle u,\psi_\omega\rangle = 1. \tag{9}$$

The evolution of the system starting with $u(Q,P;0)$ is then just the superposition of solutions to Eq. (8) with their time-dependent phases,

$$u(Q,P;t) = (1/2\pi i)\int d\omega \langle u,(\omega - L)^{-1}u\rangle \times \exp\{-i\omega t\}\psi_\omega(Q,P), \tag{10}$$

where the imaginary part of $(1/\pi i)\langle u,(\omega - L)^{-1}u\rangle$ is the relative intensity of $\psi_\omega(Q,P)$ in $u(Q,P;0)$, see also [3].

The next step in solving Liouville's equation numerically is to construct a set of functions, $u_0(Q,P)$, $u_1(Q,P)$, $u_2(Q,P)$,..., $u_n(Q,P)$,... in which Liouville's equation is tridiagonal. This can be done recur-

sively [2,3] as follows: The first of these functions $u_0(Q,P)$ is $u(Q,P;0)$, normalized with respect to the above inner product in which L is Hermitian,

$$u_0(Q,P)=u(Q,P;0)/b_0, \quad b_0=\langle u,u\rangle^{1/2}. \tag{11}$$

The subsequent elements of the tridiagonal basis are components of the solution to the three-term recurrence,

$$b_{n+1}u_{n+1}(Q,P)=(L-a_n)u_n(Q,P)-b_nu_{n-1}(Q,P), \tag{12}$$

taking $u_{-1}(Q,P)$ to be zero, and taking the parameters to be

$$a_n=\langle u_n,Lu_n\rangle, \quad \text{and}$$

$$b_n=\langle (L-a_n)u_n-b_nu_{n-1},(L-a_n)u_n-b_nu_{n-1}\rangle^{1/2}, \tag{13}$$

which make the $\{u_n(Q,P)\}$ orthonormal to one another. In this basis L is the tridiagonal matrix,

$$J=\begin{bmatrix} a_0 & b_1 & 0 & \cdots & & & 0 & \\ b_1 & a_1 & b_2 & 0 & \cdots & & & \\ 0 & b_2 & a_2 & b_3 & 0 & \cdots & & \\ \cdot & \cdot & \cdot & \cdot & \cdot & \cdot & \cdots & \\ \cdot & \cdot & \cdot & \cdot & \cdot & \cdot & \cdots & \\ \cdot & \cdot & \cdot & \cdot & \cdot & \cdot & \cdots & \\ 0 & \cdots & 0 & b_n & a_n & b_{n+1} & 0 & \cdots \\ \cdot & \cdots & \cdot & \cdot & \cdot & \cdot & \cdot & \cdots \\ \cdot & \cdots & \cdot & \cdot & \cdot & \cdot & \cdot & \cdots \\ \cdot & \cdots & \cdot & \cdot & \cdot & \cdot & \cdot & \cdots \end{bmatrix}. \tag{14}$$

The tridiagonal basis $\{u_n(Q,P)\}$ is ideal for expanding the solutions to Eq. (8) that contribute to the evolution of $u_0(Q,P)$ because the basis spans every power of L on $u_0(Q,P)$, that is, $L^nu_0(Q,P)$ for all n, and, consequently, spans the states generated by the exponential of the Liouvillian in Eq. (6). Let the expansion coefficients be $\{p_n(\omega)\}$, with $p_{-1}(\omega)$ zero because there is no $u_{-1}(Q,P)$, and $p_0(\omega)$ unity in order to satisfy Eq. (9) for the normalized $u_0(Q,P)$,

$$\psi_\omega(Q,P)=p_0(\omega)u_0(Q,P)+p_1(\omega)u_1(Q,P)+\cdots +p_n(\omega)u_n(Q,P)+\cdots. \tag{15}$$

Substituting Eq. (15) into Eq. (8), using the tridiagonal form of L, and equating the coefficients of each of the $\{u_n(Q,P)\}$ gives a recurrence relation for the coefficients,

$$b_{n+1}p_{n+1}(\omega)=(\omega-a_n)p_n(\omega)-b_np_{n-1}(\omega). \tag{16}$$

This recurrence relates three components of each solution; so, a solution is uniquely determined by two of its components, and in the absence of any boundary conditions, there are two linearly independent solutions for each value of ω, corresponding to the two linearly independent choices of two components. However, since the tridiagonal basis $\{u_n(Q,P)\}$ has no elements for n negative, the $\{p_n(\omega)\}$ are defined by the boundary condition that $p_{-1}(\omega)$ is zero, and the normalization condition in Eq. (9) makes $p_0(\omega)$ unity. These are usually called the regular orthogonal polynomials because they are polynomials in ω and can be shown to be orthogonal with respect to integration over the spectrum of the resolvent element appearing in Eq. (10), see [2].

Having shown how to calculate solutions to the time-independent Liouville equation, the next problem is that of evaluating the resolvent element, which also appears in Eq. (10). This is accomplished with the same tridiagonalization as for the stationary solutions because ω-L is also tridiagonal in this basis, and the required element is in the upper left-hand corner of the inverse. Writing the inverse element as the ratio of the cofactor and determinant of ω-L, and expanding these alternately in rows and columns yields a continued fraction expansion for

$$R(\omega)\equiv\langle u_0,(\omega-L)^{-1}u_0\rangle=1/\{\omega-a_0-b_1^2/[\omega-a_1-\cdots-b_n^2/(\omega-a_n-\cdots)\cdots]\}. \tag{17}$$

Using this continued fraction expansion for the resolvent, and taking account of the normalization of $u(Q,P;0)$ gives a numerically tractable expression for the evolution of this function,

$$u(Q,P;t)=(b_0/2\pi i)\int d\omega\psi_\omega(Q,P)R(\omega)\exp\{-i\omega t\}, \tag{18}$$

where the integral is around a contour, which encloses the real ω axis. This integral can be evaluated numerically using Gaussian quadrature [4] with nodes and weights that are the poles and residues of the finite continued fractions obtained by truncating $R(\omega)$, see further in [3].

The relationships between the singular and nonsingular parts of the integrand in Eq. (18) determine the evolution of the system. The only singularity in the exponential function is at infinite ω, and the solutions to the time-independent Liouville equation $\{\psi_\omega(P,Q)\}$ are analytic in ω, for finite P and Q, because ω is a parameter in the differential equation, Eq. (8). From the residue theorem, only singularities in the integrand of Eq. (18) contribute to its value, and those occur only in $R(\omega)$ which, according to Eq. (17), is singular for every value of ω for which there is a solution of the time-independent Liouville equation contained in $u(Q,P;0)$. The singularities in $R(\omega)$ can vary from a few isolated poles for systems such as coupled harmonic oscillators, to the case where $R(\omega)$ is analytic in the limit as ω becomes real, but with the sign of its imaginary part depending on whether the limit is taken from above or below the real axis. It is this latter case, which is of particular interest for what follows.

For real ω, the magnitude of the imaginary part of the resolvent, $|\mathrm{Im}\{R(\omega)\}|$, is also called the power spectrum, and

plays a fundamental role in the evolution of the system. Given the power spectrum, rather than the Liouvillian and the initial function $u(Q,P;0)$, the tridiagonal matrix in Eq. (14) can still be obtained by orthogonalizing polynomials with respect to $|\mathrm{Im}\{R(\omega)\}|$ [2]. From Eqs. (15) and (18), the Fourier transforms of these polynomials weighted by $|\mathrm{Im}\{R(\omega)\}|$, then gives the time-dependent coefficient of each $u_n(Q,P)$, even though the $\{u_n(Q,P)\}$ are not given. The power spectrum determines the part of the evolution, which is independent of any realization of the system.

For microscopic times, t up to where $1/t$ is comparable with the scale of the finest structure in the power spectrum, the evolution of the system is well described by the Fourier transforms of polynomials weighted by the power spectrum. Typically the nth component of the state remains small when t is so small that the cycles of $\exp\{-i\omega t\}$ are much bigger than those of $p_n(\omega)$. The nth component has greatest magnitude when the cycles are of similar size, and decreases again once the cycles of $\exp\{-i\omega t\}$ get smaller than those of $p_n(\omega)$. It is the initial part of the recurrence that determines both the general shape of the power spectrum and the early polynomials, and hence the evolution over microscopic times.

For large values of t, macroscopic times, the situation changes. The cycles in the exponential are so short that their integral over any smooth function, such as a polynomial weighted by a smooth power spectrum, goes exponentially to zero with increasing t. There is no matching of cycles, but the rate of the exponential decay is given by the location of the singularities nearest to the real ω axis in the integrand. In the cases of interest in this paper, $R(\omega)$ has no singularities in either the upper or lower halves of the ω plane or even in the limit as ω goes to the real axis from either above or below, so the polynomials and hence the initial state of the system no longer affect its evolution. The only singularities in the integrand are in the analytic continuation of $R(\omega)$ through the real ω axis from either above or below, to what is called the second sheet of $R(\omega)$. It is the imaginary parts of the ω, at which these singularities occur on the second sheet, that are the rates of exponential decay for components of the state, and determine the rates for dissipation of mechanical energy. In practical terms, the relaxation rates at macroscopic times are determined by the analytic continuation of the continued fraction in Eq. (17) from the upper half to the lower half of the ω plane where it can have singularities.

As a last note in this section on solving Liouville's equation, we should comment that the more usual approach [1] is to evolve phase-space densities, functions on phase space that are never negative, rather than more general functions. It is easy to show that when solved exactly, Liouville's equation preserves the non-negativity of densities; the problem is that it is very difficult to preserve non-negativity in approximate solutions. Because Liouville's equation is first order in all its derivatives, the evolution of a product of functions is the product of the evolutions of the individual functions. Consequently, the squared magnitude of the evolution of an arbitrary function is a density that is also a solution to Liouville's equation, and this is the way we preserve non-negativity in approximate densities. However, the functions can be multiplied by an arbitrary phase at each value of Q and P without changing the resulting density; so solutions to Liouville's equation used in this paper have a gauge symmetry that leaves the observables, the densities, invariant.

III. ANALYTIC CONTINUATION IN FREQUENCY

In the previous section we solved Liouville's equation to find the time evolution of a function on phase space; however, in order to determine the behavior at macroscopic times, we must analytically continue $R(\omega)$, defined in Eq. (17), to its second sheet. This is the second of two analytic continuations, which are central to this approach; the first being the continuation of $R(\omega)$ to its first sheet from its expansion about infinite ω. The expectation values of powers of the Liouvillian $\langle u,L^n u\rangle$, which are the moments of the power spectrum, are also coefficients of inverse powers of ω in an expansion of $R(\omega)$ about infinity [5]. This moment expansion does not necessarily converge for any values of ω, but because the power spectrum is non-negative, the moment expansion can be analytically continued to its first sheet using the continued fraction expansion of $R(\omega)$ [5]. The first sheet of $R(\omega)$ only determines the evolution of the system for microscopic times, and for macroscopic times, the continued fraction must be analytically continued to its second sheet, which is the problem addressed in this section. The method developed here is illustrated both analytically and numerically in Sec. IV.

Our approach to this problem is the analytic continuation of solutions to the recurrence in Eq. (16). Because this recurrence connects three successive components of a solution, for any complex value of ω, two components must be specified to determine the third, and hence the whole solution. In the most general case, these two initial components can be any two complex numbers, so the space of solutions has two complex dimensions. One of these two, complex degrees of freedom may be taken to be a complex normalizing factor, which multiplies every component of a solution. This leaves a single important degree of freedom, which is the ratio of a pair of components. There are two linearly independent polynomial solutions to the recurrence, the regular orthogonal polynomials $\{p_n(\omega)\}$, whose -1st and 0th components are conventionally taken to be zero and unity, respectively, and the irregular polynomials $\{q_n(\omega)\}$, whose 0th and 1st components are taken to be zero and unity. When the recurrence is infinite, we show below that $R(\omega)$ is related to the solution that goes to zero fastest as n goes to infinity in the recurrence, the solution whose ratios of successive components has the smallest magnitude at infinity, which for each ω we denote by $\{c_n(\omega)\}$.

The continued fraction expansion in Eq. (17) can be viewed as a relation between the ratios of successive components of a solution to the recurrence. Using $\{c_n(\omega)\}$ as an example, the recurrence for $n=0$ gives

$$b_1 c_1(\omega)=(\omega-a_0)c_0(\omega)-b_0 c_{-1}(\omega), \tag{19}$$

which can be rearranged as a fraction,

$$c_0(\omega)/[b_0 c_{-1}(\omega)]=1/[\omega-a_0-b_1 c_1(\omega)/c_0(\omega)]. \tag{20}$$

The recurrence for $n=1$ can be similarly rearranged to give a fraction for $c_1(\omega)/[b_1 c_0(\omega)]$ in terms of $c_2(\omega)/[b_2 c_1(\omega)]$ and so on. Linking these relations together gives a continued fraction relation between $c_0(\omega)/[b_0 c_{-1}(\omega)]$ and $c_{n+1}(\omega)/[b_{n+1}c_n(\omega)]$ for any n.

Shohat and Tamarkin [5] show that under conditions that apply to this work, and for ω not real, the continued fraction in Eq. (17) converges with increasing number of levels. In terms of the above relation between ratios of successive components of a solution, as n goes to infinity, the continued fraction takes as its value the ratio of successive components of just one of the solutions to the recurrence. This must be the solution that depends least on what happens at large n, or, in other words, it is the solution that goes to zero most rapidly with increasing n. Because the fraction converges, the most convergent solution is unique for ω not real. This result can be seen informally by noting that a continued fraction is naturally evaluated from the bottom up, corresponding to evaluation of the recurrence, starting at large n and working backwards to $n=0$. The reverse evaluation of a recurrence is dominated by the solution, which increases most rapidly in magnitude as n decreases. Since solutions can be generated by recurring in either direction, the one that increases in magnitude most rapidly as n decreases is the one that converges to zero most rapidly as n increases.

For the systems studied below, the a_n are all zero, and b_n are either proportional to n, or become proportional to n for n large. For this reason we study the recurrence in which b_n is αn with α greater than 0. As for related second-order differential equations, we try a solution containing only exponential and algebraic singularities at infinite n,

$$c_n(\omega)=g_n(\omega)A(\omega)^n n^{B(\omega)}, \tag{21}$$

where $g_n(\omega)$ is analytic at infinite n, meaning that it goes smoothly to a constant as n goes to infinity. When this trial solution is substituted into the recurrence, it becomes

$$\begin{aligned}\alpha(n+1)A(\omega)^{n+1}(n+1)^{B(\omega)}g_{n+1}(\omega)&\\ =\omega A(\omega)^n n^{B(\omega)}g_n(\omega)&\\ -\alpha n A(\omega)^{n-1}(n-1)^{B(\omega)}g_{n-1}(\omega).&\end{aligned} \tag{22}$$

Requiring that $g_n(\omega)$ contain no positive powers of n near $n=\infty$ leads to two possible solutions,

$$A(\omega)=\pm i, \quad \text{and} \quad B(\omega)=-(1\pm i\omega/\alpha)/2, \tag{23}$$

distinguished by taking either the upper or lower signs in both expressions. Each choice of sign gives a linearly independent solution, and we could proceed to expand $g_n(\omega)$ in powers of $1/n$, but the exponential and algebraic singularities of the solution, $A(\omega)$ and $B(\omega)$, turn out to be all that is needed from this analysis. For ω in the upper half plane, it is clear that the lower choice of sign gives the most convergent solution $\{c_n(\omega)\}$, which is related to the continued fraction by Eq. (20). The choice of the lower signs for ω in the lower half plane gives the most divergent solution $\{d_n(\omega)\}$, one which grows faster, or at least shrinks slower, than any other as n goes to infinity. For ω not real, this most divergent solution is also unique for the same reason that the most convergent solution is unique.

Since $A(\omega)$ has unit modulus, and since at infinity in n $\{g_n(\omega)\}$ generally goes to a constant, which can be taken to be unity, the convergence or divergence of a solution to the recurrence depends on the real part of the exponent $B(\omega)$. The most convergent solution for a given ω has $B(\omega)$ with a real part that is greater than $-\frac{1}{2}$, and the most divergent solution has $B(\omega)$ with a real part less than $-\frac{1}{2}$. As ω goes through the real axis, the real part of $B(\omega)$ goes from one side of $-\frac{1}{2}$ to the other, and the most convergent and divergent solutions interchange. This crossover between convergence and divergence is similar to that displayed by second-order differential equations. As in the case of differential equations the crossover of the analytic part of the solution can be complicated; however, such complications are unnecessary for the purposes of this paper provided that the most divergent solution can be constructed for each ω off the real axis. Since Eq. (20) relates the continued fraction to the most convergent solution, which continues to the most divergent solution, the second sheet value of the continued fraction is

$$S(\omega)=d_0(\omega)/[b_0 d_1(\omega)], \tag{24}$$

where $\{d_n(\omega)\}$ is the most divergent solution to the recurrence.

In order to evaluate the second sheet of the continued fraction, only the most divergent solution to the recurrence is required, and because the singular factors in this solution are given by Eq. (23), only the analytic factor $\{g_n(\omega)\}$ remains to be determined numerically. However, an expansion of $\{g_n(\omega)\}$ in inverse powers of n converges very poorly for small n. A numerically stable approach is to express $S(\omega)$ as a ratio of components of the most convergent solution for large n, and calculate these by subtracting fits to the most divergent solutions from polynomial solutions to the recurrence. The first step in deriving such an expression is to expand the regular polynomial solutions $[p_{-1}(\omega)=0$ and $p_0(\omega)=1]$ and irregular polynomial solutions $[q_0(\omega)=0$ and $q_1(\omega)=1]$ in the most convergent and divergent solutions,

$$\begin{aligned}q_n(\omega)&=q_c(\omega)c_n(\omega)+q_d(\omega)d_n(\omega), \quad \text{and}\\ p_n(\omega)&=p_c(\omega)c_n(\omega)+p_d(\omega)d_n(\omega),\end{aligned} \tag{25}$$

where $q_c(\omega)$, $q_d(\omega)$, $p_c(\omega)$, and $p_d(\omega)$ are coefficients that depend only on ω and are determined by the initial conditions for the two kinds of polynomials. There are only two linearly independent solutions to the recurrence for each value of ω; so only two terms are needed for each expression. Next, eliminate $c_n(\omega)$ from the above two equations, solve for $d_n(\omega)$, and substitute this into Eq. (24) to get

$$S(\omega)=q_c(\omega)/[b_1 p_c(\omega)]. \tag{26}$$

This expresses the second sheet of the continued fraction in terms of the ratio of $q_c(\omega)$ to $b_1 p_c(\omega)$ that is the ratio of coefficients of $c_n(\omega)$ in $q_n(\omega)$ and $b_1 p_n(\omega)$ in Eq. (25). This is just the ratio of the convergent components of $q_n(\omega)$

and $b_1 p_n(\omega)$, or what is left when the divergent components are subtracted from $q_n(\omega)$ and $b_1 p_n(\omega)$.

The polynomials $\{q_n(\omega)\}$ and $\{b_1 p_n(\omega)\}$ defined above are dominated by their most divergent components as n increases, and for ω in the upper half plane; this part of each can be expanded in the form $(-i)^n n^{-(1-i\omega/\alpha)/2} g_n(\omega)$, Eq. (21), where $g_n(\omega)$ is analytic in n at infinity. In order to approximate $q_c(\omega)c_n(\omega)$ and $b_1 p_c(\omega)c_n(\omega)$, we fit $q_0(\omega),\ldots,q_{n-1}(\omega)$ and $b_1 p_0(\omega),\ldots,b_1 p_{n-1}(\omega)$ to Eq. (21), in each case expanding $\{g_n(\omega)\}$ in n nonpositive powers of $n+1$. These fits are used to estimate the divergent parts of $q_n(\omega)$ and $b_1 p_n(\omega)$ that are subtracted from them to produce approximate values of $q_c(\omega)c_n(\omega)$ and $b_1 p_c(\omega)c_n(\omega)$. These latter quantities are substituted into Eq. (26) where $c_n(\omega)$ in the numerator cancels $c_n(\omega)$ in the denominator to give $S(\omega)$, the second sheet of the continued fraction. As n increases this approximation improves until rounding error limits the significance of the differences between $q_n(\omega)$ or $b_1 p_n(\omega)$ and their most divergent components. The dependence of errors on n is illustrated in Sec. IV.

The second sheet of the continued fraction may be interpreted physically as the complex admittance (the inverse of impedence) of the system. The poles on the second sheet occur at complex ω at which the system absorbs energy without reflection and dissipates that energy if ω has an imaginary part. The zeros occur at ω for which the system is perfectly reflective, and at ω, which are neither zeros nor poles, the system absorbs some energy and reflects the rest. The eigenfunctions of the Liouvillian corresponding to features in complex ω give the densities in Q and P for which the system absorbs, dissipates, or reflects at ω.

The analytic continuation of $R(\omega)$ is only possible if the two extremal solutions to the recurrence continue into one another on the real ω axis, and we show here that this happens only if there are traveling-wave solutions for real ω. The recurrence in Eq. (16) always has two linearly independent solutions, which for most ω can be taken to be the most convergent and the most divergent as above. In special cases, the divergent and convergent solutions can become degenerate in the sense that all solutions go to a constant magnitude for n large. This degeneracy is necessary for one extremal solution to continue into the other as ω varies; otherwise, the continuation would be nonanalytic at the value of ω where limiting behavior of the two solutions interchanged without becoming identical. The convergence of the continued fraction for all ω except possibly on the real ω axis [5] shows that the converging solution is unique except possibly on the real ω axis, and hence that there is no degeneracy except possibly on the real ω axis. So, it is only along the real ω axis that the extremal solutions can continue into one another, and only there can the solutions be degenerate. For real ω at which the solutions are degenerate, we can construct two independent, real (because the coefficients in the recurrence are all real) solutions to the recurrence whose magnitudes go to the same value at infinite n. The traveling wave is the complex combination of these two solutions, which is in quadrature in the limit of infinite n. Conversely, if there are no traveling waves, then there is no degeneracy, and hence no analytic continuation.

The physical significance of the traveling waves is that they allow the initial state of the system to propagate to $u_n(Q,P)$ for infinite n, corresponding to functions of infinite wave number with respect to Q and P. A further interpretation of this process is that a density that varies slowly with Q or P evolves, due to the nonlinear forces, into one which varies ever more rapidly with Q and P and finally into one that evolves infinitely rapidly with Q and P. When the wave numbers of the density variations become infinite, these variations become microscopic so the mechanical energy they contained has been dissipated by some microscopic process, and the system has achieved equilibrium.

Another property of traveling waves is that they belong to bands defined by the intervals of ω over which the complex phase difference between successive components varies from zero to π, in the limit as n goes to infinity. For example, the traveling-wave solutions in Eq. (22) go to a limiting phase difference of $\pi/2$ for all real ω, and so the band extends over the entire real ω axis. If b_n had been constant rather than increasing in n, the band would have extended in ω from $-2b_n$ to $2b_n$, with the limiting phase zero at $2b_n$ and π at $-2b_n$.

The trial solution adopted in Eq. (21) has an exponential singularity at infinite n, but such simple singularities occur only for recurrences in which a_n goes to a constant and b_n becomes linear in n as n goes to infinity. When the recurrence parameters have more complicated behavior, for example in electronic structure calculations where multiple bands are present [6], the singularity at infinity in the solution to the recurrence is not a simple exponential, and there does not seem to be any form comparable to Eq. (21). The same problems arise in ordinary differential equations with irregular singularities at infinity, see [7], where simple exponential singularities are the only ones for which solutions can be expanded about infinity.

IV. THE INVERTED OSCILLATOR

The inverted oscillator is the simplest system whose solutions to Newton's equations, Eqs. (1) and (2), diverge exponentially in phase space, a characteristic of chaotic motion and related to the existence of traveling-wave solutions to Liouville's equation. The inverted oscillator consists of a particle with mass M moving in a quadratic potential,

$$U(x) = -KX^2/2, \tag{27}$$

where X is displacement. Despite the absence of oscillatory motion, there is a natural phase velocity,

$$\omega_0 = (K/M)^{1/2}, \tag{28}$$

which sets a time scale. Since Newton's equations can be solved analytically for this system, the trajectories of the particle can be compared directly with results from the methods developed above.

Liouville's equation can also be solved both analytically and numerically for this system [3,8]. In terms of ω_0, the Liouvillian is

$$L = -i\omega_0[y\,\partial/\partial x + x\,\partial/\partial y], \tag{29}$$

where x is the displacement scaled by any unit of distance, and y is the velocity of the particle scaled by the same unit of

distance and divided by ω_0. Following Haydock and Kim [3] and the procedure described in Sec. II, we tridiagonalize L analytically starting with an initial distribution, chosen to be Gaussian. Let u_0 be the normalized Gaussian,

$$u_0 = \exp\{-(x^2+y^2)/2\}/\pi. \tag{30}$$

It can then be shown that the rest of the tridiagonal basis consists of the functions,

$$u_n = (i)^n h_n(x) h_n(y) u_0, \tag{31}$$

where $h_n(x)$ is the nth Hermite polynomial, normalized to $\sqrt{\pi}$ with respect to integration over $\exp\{-x^2\}$. The recurrence parameters are

$$a_n = 0 \quad \text{and} \quad b_n = n\omega_0, \tag{32}$$

which is just the kind of recurrence analyzed in Sec. III.

More generally, the Liouvillian for the inverted oscillator is tridiagonal in the isotropic oscillator functions,

$$u_{k,m} = (i)^k h_k(x) h_m(y) \exp\{-(x^2+y^2)/2\}/\pi, \tag{33}$$

which form a complete set of functions on the phase space of this system when k and m take values from 0, 1, ... The tridiagonal matrix elements are given by

$$Lu_{k,m} = \omega_0\{[(k+1)(m+1)]^{1/2} u_{k+1,m+1} + (km)^{1/2} u_{k-1,m-1}\}, \tag{34}$$

and each tridiagonal subspace starts with the function $u_{0,m}$, or $u_{k,0}$. The recurrences for stationary solutions to Liouville's equation are satisfied by Meixner polynomials of the second kind [9] of which the mth set of polynomials are orthogonal with respect to integration over real ω with the weight distribution,

$$w_m(\omega) = 2^m \Gamma((m + i\omega/\omega_0 + 1)/2) \times \Gamma((m - i\omega/\omega_0 + 1)/2)/(2\pi m!), \tag{35}$$

where $\Gamma(z)$ is the gamma function. These weight distributions are also the power spectra of the motion of the inverted oscillator for the initial state $u_{0,m}$. In the case where u_0 is given by Eq. (30) the relations between the gamma function and hyperbolic functions make this weight distribution $\{2\omega_0 \cosh[\pi\omega/(2\omega_0)]\}^{-1}$.

The continued fractions for the inverted oscillator can be analytically continued by inspection. The weight distributions in Eq. (35) have poles along the imaginary ω axis at either odd or even integer multiples of $i\omega_0$ starting at $\pm(n+1)i\omega_0$. The property that the continued fraction $R(\omega)$ has no poles or zeros other than on the real ω axis and that it varies as $1/\omega$ at infinity, uniquely determines its analytic continuation, $R_n^+(\omega)$ for $w_n(\omega)$ in Eq. (35). For n zero,

$$R_0^+(\omega) = \beta((1 - i\omega/\omega_0)/2)/(2i), \tag{36}$$

for n one,

$$R_1^+(\omega) = i - \omega\beta(-i\omega/2\omega_0)/2, \tag{37}$$

and in general,

$$R_n^+(\omega) = \begin{cases} s_n(\omega) + (1 - i\omega/\omega_0)(3 - i\omega/\omega_0)\cdots(n-1-i\omega/\omega_0)\beta(1/2 - \omega i/2\omega_0)/(2in!) & \text{for } n \text{ even}, \\ s_n(\omega) - (\omega/\omega_0)(2 - i\omega/\omega_0)\cdots(n-1-i\omega/\omega_0)\beta(-\omega i/2\omega_0)/(2n!) & \text{for } n \text{ odd}, \end{cases} \tag{38}$$

where the function $\beta(x)$ is defined in Gradshteyn and Ryzhik [10], and the $s_n(\omega)$ are polynomials in ω, which cancel the polynomial behavior of the second term at infinity in the upper half plane.

The above analytic forms for the power spectrum, Eq. (35), and the second sheet of the continued fraction, Eq. (36), serve as a check on the numerical methods for obtaining these quantities. Since numerical errors in tridiagonalizing operators are well understood [11], we begin the numerical studies with the exact tridiagonalization given in Eq. (32) and solve Eq. (16) numerically to obtain its extremal solutions, convergent and divergent, for parts of the real and imaginary ω axes. For ω real, the imaginary parts of the two solutions give the power spectrum, and for ω imaginary, the two solutions combine to give the analytic continuation of the power spectrum to imaginary frequencies.

Figure 1 shows part of the normalized power spectrum for $u_{0,0}$, calculated using Eq. (25) with an expansion of $d_n(\omega)$ to order $(1/n)^9$ from the 10×10 submatrix in the upper left-hand corner of Eq. (14). The figure includes only the positive frequencies from 0 to 5, in units of ω_0 because the spectrum is symmetric about zero. The largest error in the range shown is about $1.45\times10^{-9}/\omega_0$ at ω equals zero, while the smallest error is about $10^{-12}/\omega_0$. There is no indication in the data that the magnitude of the errors change systematically outside the range shown.

Figure 2 shows errors in the reciprocal of the analytic continuation of the power spectrum along part of the imaginary ω axis. As can be seen from Eq. (35), $w_0(\omega)$ has poles at $\pm i\omega_0$, $\pm 3i\omega_0$, and so on, but no zeros. In order to make sense of the error near the poles of $w_0(\omega)$, we plot the error in $1/w_0(\omega)$, which has zeros at $\pm i\omega_0$, $\pm 3i\omega_0$, and so on. The numerical continuation of the power spectrum is very sensitive to the order of the approximation, so we have plotted the errors for expansions of order $(1/n)^5$, $(1/n)^7$, and $(1/n)^9$ for the solutions to the recurrence, and these expansions were obtained, respectively, from the 5×5 submatrix to the 9×9 submatrix in the upper left-hand corner of Eq. (14). The most remarkable feature of the calculations behind this figure is that where the approximate spectra have poles, the locations of the poles are accurate to order $10^{-13}\omega_0$, essentially the full precision of the calculation. This phenomena

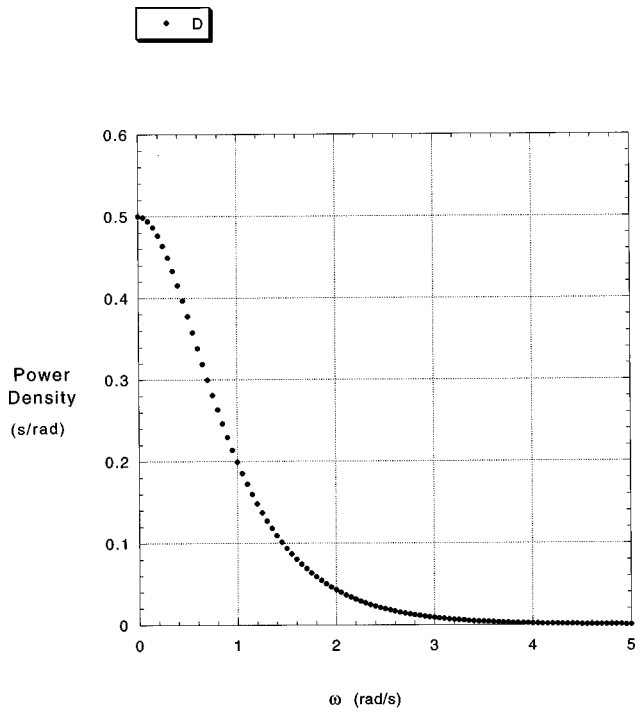

FIG. 1. The power spectrum for the inverted oscillator starting from a Gaussian distribution in phase space.

appears similar to the Lanczos' phenomenon [12] in which, as the order of approximation increases, successive eigenvalues, in this case of the Liouvillian, converge to full arithmetic precision despite other eigenvalues remaining unconverged. Increasing the order of approximation beyond $(1/n)^9$ leads to no further reductions in errors because at this level

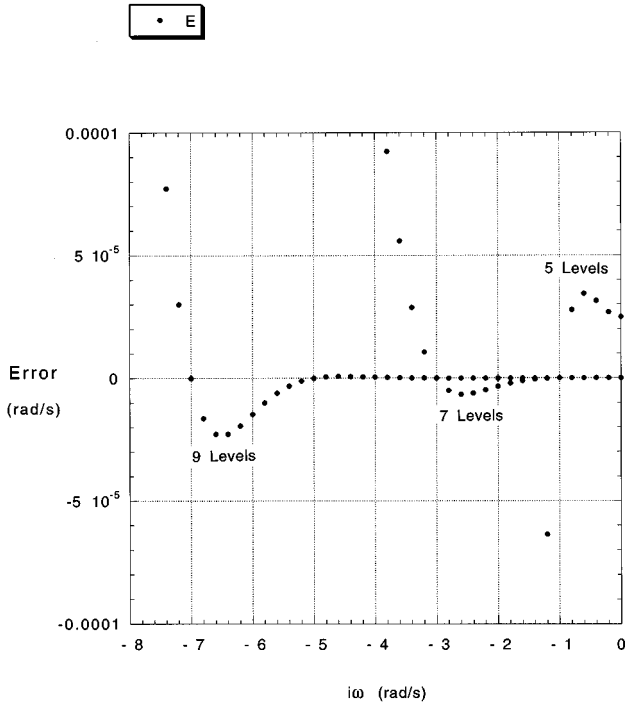

FIG. 2. Errors in the reciprocal of the power spectrum for the inverted oscillator, numerically continued to the negative imaginary frequency axis for different orders of approximation.

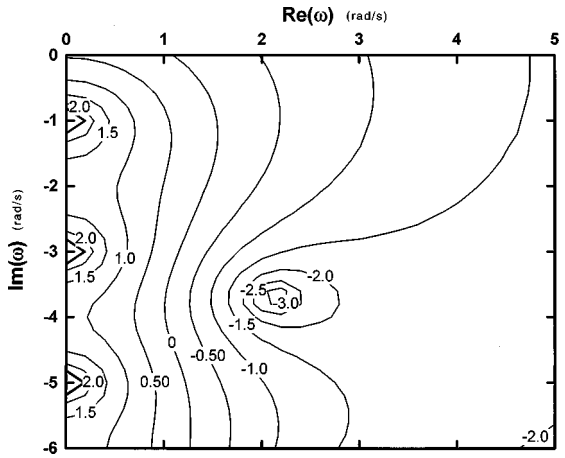

FIG. 3. Contours of constant magnitude in the analytic continuation of the continued fraction for the inverted oscillator.

of approximation the errors are determined by the precision of the arithmetic used, as discussed at the end of Sec. III.

Figure 3 displays contours equally spaced in the logarithm of $|R(\omega)|$, continued into the complex plane just below the real axis. Like the spectrum, the continued fraction and its second sheet are symmetric about the imaginary ω axis, so only ω with positive real parts are included. The most significant features are the first three poles of the continuation, on the negative imaginary ω axis at $-i\omega_0$, $-3i\omega_0$, and $-5i\omega_0$. There is also a zero of the continuation near the center of the figure. The presence of a zero in that part of the complex ω plane is consistent with the partial fraction expansion of the β function [10], but we do not know of any study of the zeros of this function.

V. A CHARGED PARTICLE IN A PERIODIC MAGNETIC FIELD

The transverse motion of a classical charged particle in an inhomogeneous, periodic magnetic field is particularly simple because when all the unit cells of the lattice are mapped onto a single cell, the phase space of the particle is a three torus, two of whose dimensions are position in the cell and the third is the angle of the velocity vector. Take X, Y, and Z to be a right-handed system of Cartesian coordinates, and let the field be $-B[\cos(X/a)+\cos(Y/a)]$ times a unit vector in the Z direction. A particle of charge Q and mass M moves with speed V in the X-Y plane. Newton's equations for this system are

$$dX/dt = V\cos\theta,$$

$$dY/dt = V\sin\theta,$$

$$d\theta/dt = QB[\cos(X/a)+\cos(Y/a)]/M, \tag{39}$$

where θ is the angle the velocity vector makes with the X axis. The phase space of this system is three-dimensional because the magnitude of the velocity of the particle never changes, just its direction.

The Liouvillian for this system is

TABLE I. Tridiagonal matrix elements for the charged particle in a periodic magnetic field.

$a_0 = 0.000\,000\,00$	$b_1 = 1.000\,000\,00$
$a_1 = 0.000\,000\,00$	$b_2 = 1.322\,875\,98$
$a_2 = 0.000\,000\,00$	$b_3 = 1.700\,839\,04$
$a_3 = 0.000\,000\,00$	$b_4 = 2.536\,593\,44$
$a_4 = 0.000\,000\,00$	$b_5 = 2.796\,948\,43$
$a_5 = 0.000\,000\,00$	$b_6 = 3.547\,017\,10$
$a_6 = 0.000\,000\,00$	$b_7 = 4.088\,612\,56$
$a_7 = 0.000\,000\,00$	$b_8 = 4.617\,911\,34$
$a_8 = 0.000\,000\,00$	$b_9 = 5.535\,735\,13$
$a_9 = 0.000\,000\,00$	$b_{10} = 6.030\,636\,79$

$$L = -i[v\cos\theta\partial/\partial x + v\sin\theta\partial/\partial y + (QB/M)(\cos x + \cos y)\partial/\partial\theta], \tag{40}$$

where v, x, and y are V/a, X/a, and Y/a, respectively. The natural choice of basis functions for this Liouvillian are the plane waves on the reciprocal lattice,

$$\phi_{j,k,n} = \exp\{i(jx + ky + n\theta)\}, \tag{41}$$

where j, k, and n vary over the integers. The action of the Liouvillian on $\phi_{j,k,n}$ gives

$$L\phi_{j,k,n} = (v/2)(j - ik)\phi_{j,k,n+1} + (v/2)(j + ik)\phi_{j,k,n-1} + [QB/(2M)]n(\phi_{j+1,k,n} + \phi_{j-1,k,n} + \phi_{j,k+1,n} + \phi_{j,k-1,n}). \tag{42}$$

This is similar to electronic band theory in that a reciprocal lattice of plane waves is coupled together, but it differs in that the matrix elements grow linearly with wave number. Note that $\phi_{0,0,0}$ is invariant because it is just the constant density in phase space.

A convenient choice of starting state is to make u_0 equal $\phi_{0,0,1}$, which is a function whose phase varies with the angle of the velocity. Constructing the solution to the recurrence in Eqs. (12) and (13), it is easy to see that the a_n are exactly zero, but that the b_n can only be calculated approximately. Carrying out the recursive tridiagonalization of L in the case where v and QB/M are both unity, produces the b_n given in Table I.

We have calculated b_n for n up to 400, and find that b_n becomes linear in n with a coefficient that we have fit to the coefficient α, which appears in Eq. (23). Another way to see how b_n grows with n is to note that the matrix elements of the plane-wave representation of L also increase linearly with the band indices. This leads to a linear increase in b_n with a coefficient, which is similar to the one obtained by fitting.

Figure 4 shows the power spectrum obtained from this continued fraction and Fig. 5 shows a contour map for the analytic continuation of this fraction over a portion of the frequency plane similar to that in Fig. 1., calculated numerically by the method described in Sec. III. Although the recurrence produced by the periodic magnet is similar to that of the inverted oscillator, the relaxation processes seem very different. While the power spectrum of the inverted oscillator has only a central peak, the periodic magnet has a resonance

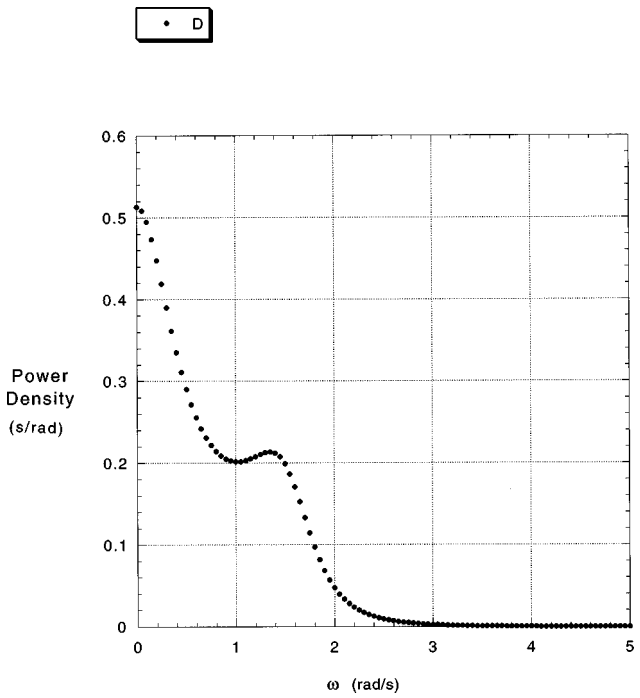

FIG. 4. The power spectrum for the charged particle in a periodic magnetic field.

at about 1.4 frequency units, associated with some nearly periodic motion of the charge such as a cyclotron orbit. The same resonance shows up as a pole in the continuation of the fraction, with an ω whose real part is about 1.5 and whose imaginary part is about 0.4.

The inverted oscillator had an infinite hierarchy of relaxation times, which produce poles at the odd integers of the negative imaginary ω axis on the second sheet, while the periodic magnet only produces one, at least within 30 frequency units of the origin. This makes sense because the linear forces of the inverted oscillator leave different harmonics uncoupled allowing them to have different relaxation times, and the periodic magnet couples all modes and gives

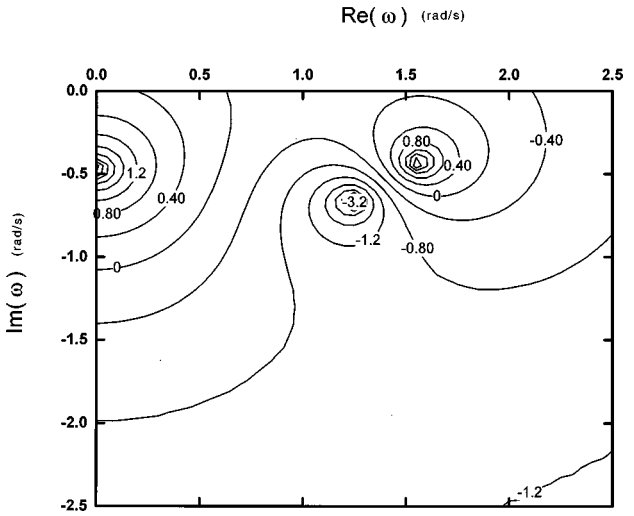

FIG. 5. Contours of constant magnitude in the analytic continuation of the continued fraction for the charged particle in a periodic magnetic field.

them the same relaxation time. In order for the power spectrum to decrease exponentially at infinite frequency, there must be an infinite number of poles and zeros on the second sheet. It seems that in the case of the periodic magnet, only one of the poles is on the negative ω axis.

VI. MORE PARTICLES, CHAOS, AND DISSIPATION

The first conclusion, which we wish to draw from this paper is that solution of Liouville's equation is a practical, even efficient, method for determining the motion of classical systems. For microscopic times, the approach presented above gives results comparable with other methods, but in conjunction with the analytical continuation of the continued fraction, it allows the determination of macroscopic relaxation times, which are difficult to calculate by other methods. In addition to its practical advantages, this approach has a mathematical foundation, which gives error estimates and establishes a range of validity.

In comparison with other methods, it is appropriate to ask how the computational effort scales with the size of the system. In each of the above examples there is a single particle whose motion changes because of the presence of forces. In most problems of interest, there are many particles whose motion is determined by forces due to interactions between them. While we leave the problem of many interacting particles for future work, in this section we point out the similarities between the problem of one particle in a force field, and that of several interacting particles.

The most important point is that the computational effort required to solve Liouville's equation does not depend on the number of interacting particles because, as we shall show, the Liouvillian operator is infinite dimensional for any number of particles. Phase space for one particle has coordinates, which are the position and momentum of the particle. For N particles, the phase space has dimension $6N$ if each particle is free to move in three dimensions: three position coordinates for each particle, and three components of momentum for each particle. However, the Liouvillian operator acts on the space of functions on phase space, not the coordinates themselves, so whether there are one, two, or N particles, there are infinitely many independent functions of the position and momentum coordinates. In other words, the Liouvillian is an infinite dimensional operator as was shown in the above, single-particle examples, and it remains so for systems of several particles.

The only way the problem changes when there are more particles is that the basic functions used to represent the Liouvillian acquire more indices. For the periodic magnet, the phase space is three-dimensional, and for N particles constrained to move in a plane with similar speed-conserving interactions, the phase space is $3N$ dimensional. A similar basis of plane waves for this phase space has $3N$ indices corresponding to the components of the wave number in each of the $3N$ directions in phase space. The procedure for constructing a tridiagonal basis out of combinations of the plane waves is the same; there are simply more plane waves combining to form each element of the tridiagonal basis. A starting state for the tridiagonalization, similar to the one used above, is constant in all coordinates except the direction of the velocity of one particle. The only difference in the resulting recurrence is that for small n the b_n are larger reflecting the increased number of ways the initial disturbance can distribute over the N particles. The power spectrum increases in width with the number of interacting particles; so the computational effort required to resolve a feature of fixed width in frequency also increases with the number of particles, but it is only this and related single-particle-like quantities, which require more effort to calculate for more particles. The macroscopic properties of the system, the relaxation rates at long times, do not depend on the motion of individual particles and so require the same computational effort independent of the number of particles, consistent with the fact that relaxation rates in real systems are independent of the system size, once it is larger than some correlation length.

The second and more general conclusion we wish to draw from this paper is that macroscopic dissipation depends on microscopic chaos. The way by which motion is dominated at long times by singularities with complex frequencies depends on the analyticity of autocorrelation functions for real frequencies that depends in turn on traveling-wave solutions to Liouville's equation, and the traveling-wave solutions depend on the lack of any cyclic component to the motion. In a finite system, the only way functions can generate an infinite dimensional space is with unbounded increase in wave number. If the functions increase in wave number, the trajectories of the system must evolve into ever finer tangles, which is the link between chaos and dissipation.

ACKNOWLEDGMENTS

The authors acknowledge assistance from Guna Rajagopal. This paper was supported by the National Science Foundation's Office of Science and Technology Infrastructure under Grant No. STI-9413532.

[1] I. Prigogine, *Non-Equilibrium Statistical Mechanics* (Interscience, New York, 1962).

[2] Roger Haydock, *Solid State Physics* (Academic, London, 1980), Vol. 35, pp. 215–294.

[3] Roger Haydock and David B. Kim, Comput. Phys. Commun. **87**, 396 (1995).

[4] For example, see W. H. Press *et al.*, *Numerical Recipes* (Cambridge University Press, Cambridge, 1986).

[5] J. A. Shohat and J. D. Tamarkin, *The Classical Moment Problem*, Math. Surv. I. rev. ed. (American Mathematical Society, Providene, RI, 1950).

[6] G. Allan, in *The Recursion Method and its Applications*, edited by D. G. Pettifor and D. L. Weaire (Springer, Heidelberg, 1985), p. 61.

[7] E. L. Ince, *Ordinary Differential Equations* (Dover, New York, 1944).

[8] P. Gaspard, G. Nicolis, A. Provata, and S. Tasaki, Phys. Rev. E **51**, 74 (1995).
[9] T. S. Chihara, *An Introduction to Orthogonal Polynomials* (Gordon and Breach, New York, 1978).
[10] I. S. Gradshteyn and I. M. Ryzhik, *Table of Integrals, Series, and Products* (Academic, New York, 1980), Chap. 8, ¶ 37.
[11] Roger Haydock and Ronald L. Te, Phys. Rev. B **57**, 296 (1998).
[12] B. N. Parlett, *The Symmetric Eigenvalue Problem* (Prentice-Hall, Englewood Cliffs, NJ, 1980).